WACQT | Wallenberg Centre for Quantum Technology

OpenSuperQ

Experimenting with Superconducting Quantum Processors

Liangyu Chen

CHALMERS Team

Tahereh Abad
Anuj Aggarwal
Janka Biznárová
Liangyu Chen
Miroslav Dobsicek
Jorge Fernández-Pendás
Simon Pettersson Fors
Göran Johansson
Sandoko Kosen
Christian Križan
Hang-Xi Li
Eleftherios Moschandreou
Andreas Nylander
Amr Osman
Robert Rehammar
Marcus Rommel
Anita Fadavi Roudsari
Daryoush Shiri
Tom Vethaak
Christopher Warren
Alexey Zadorozhko
Anton Frisk Kockum
Giovanna Tancredi
Per Delsing
Jonas Bylander

VTT Team

Marco Caputo
Leif Grönberg
Kestutis Grigoras
Joonas Govenius

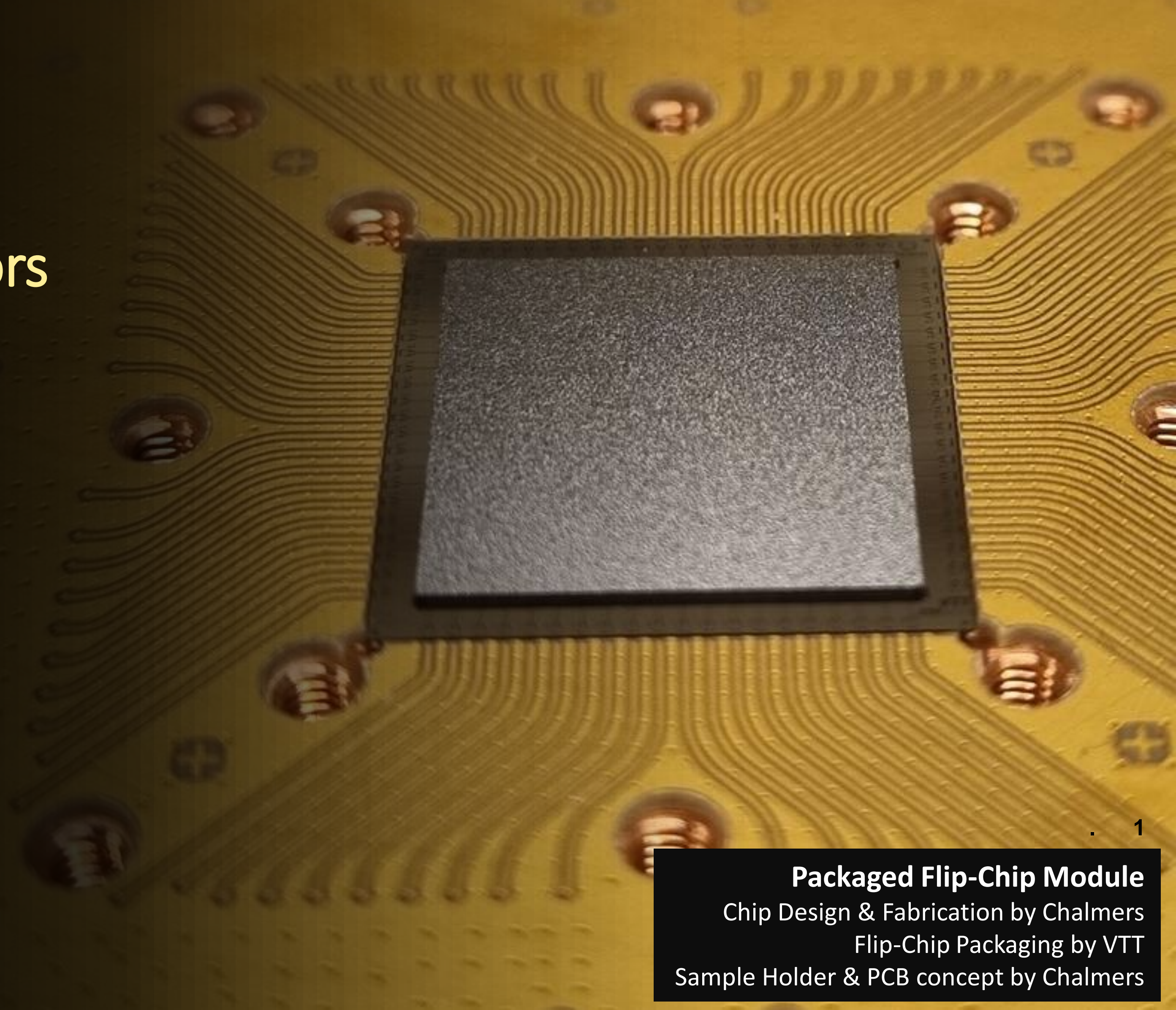

Packaged Flip-Chip Module
Chip Design & Fabrication by Chalmers
Flip-Chip Packaging by VTT
Sample Holder & PCB concept by Chalmers

Basic elements

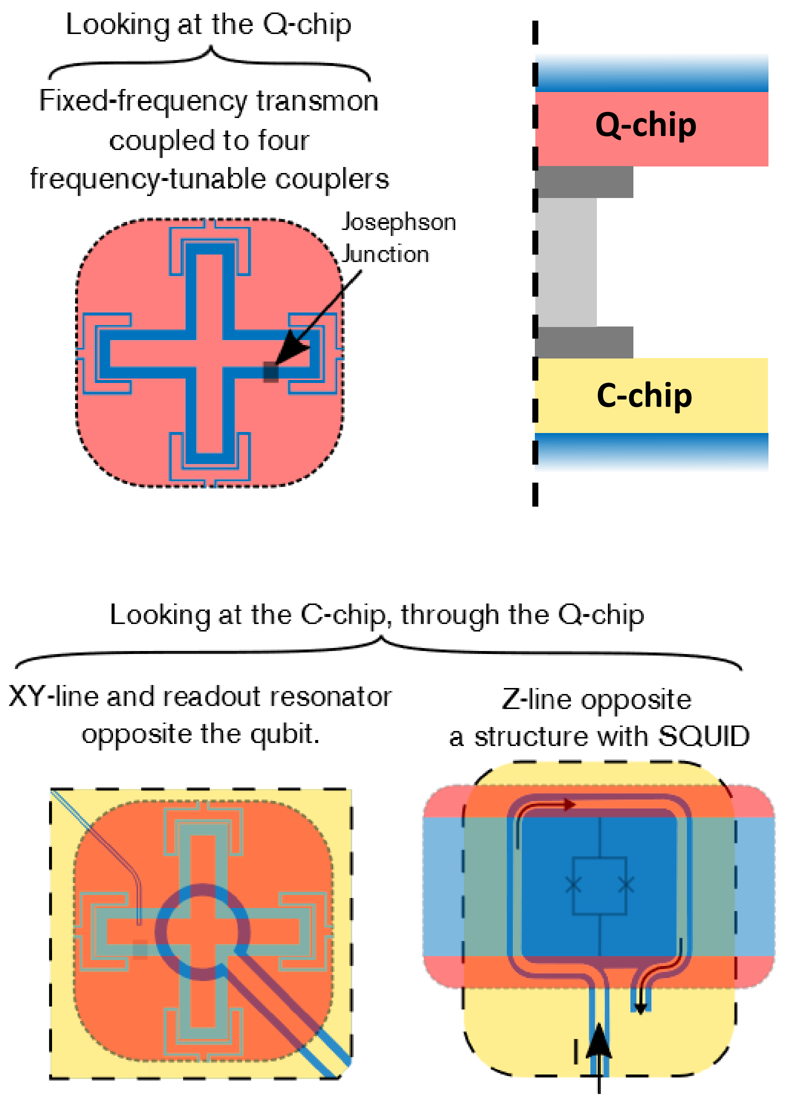

Routing corridor between two qubit rows

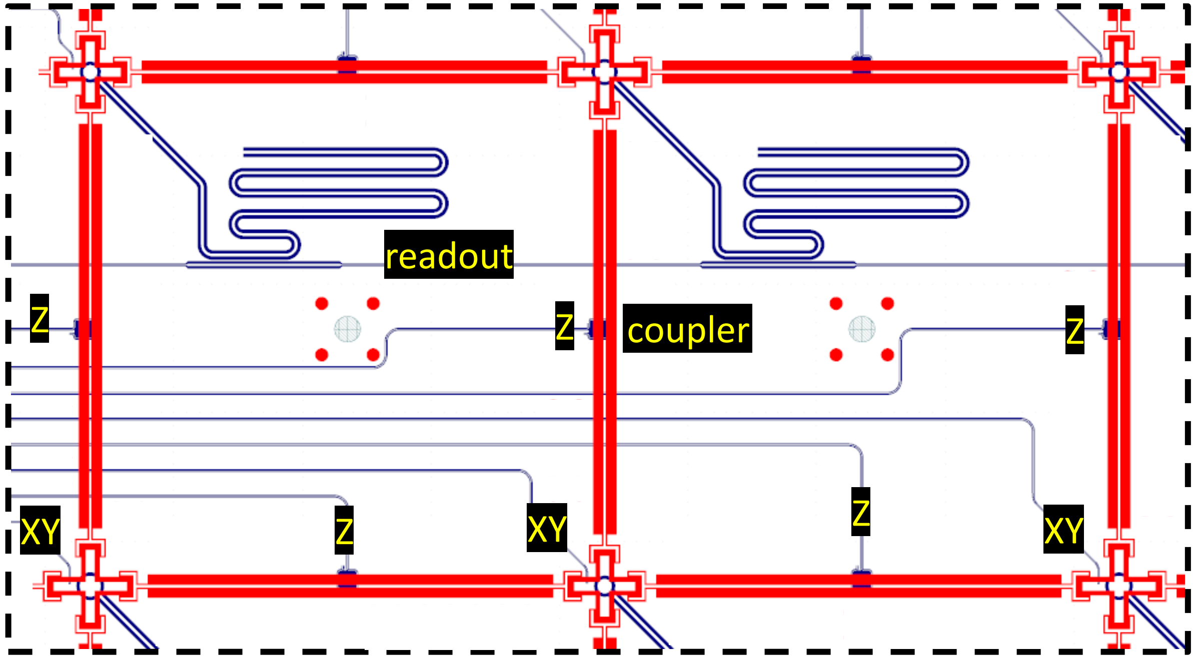

Automation of design and simulation

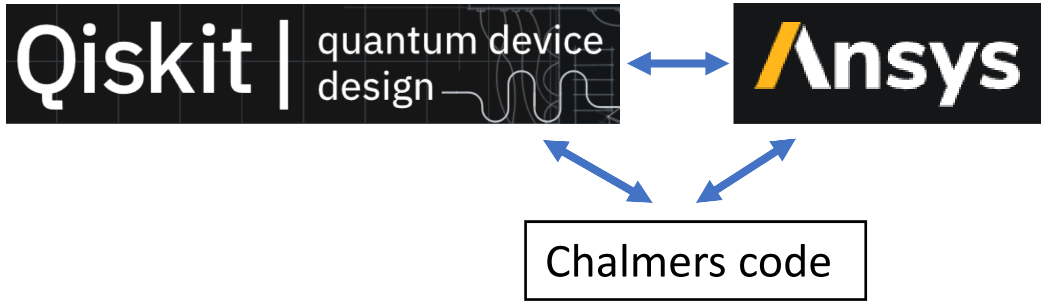

1.1 General properties of quantum measurements

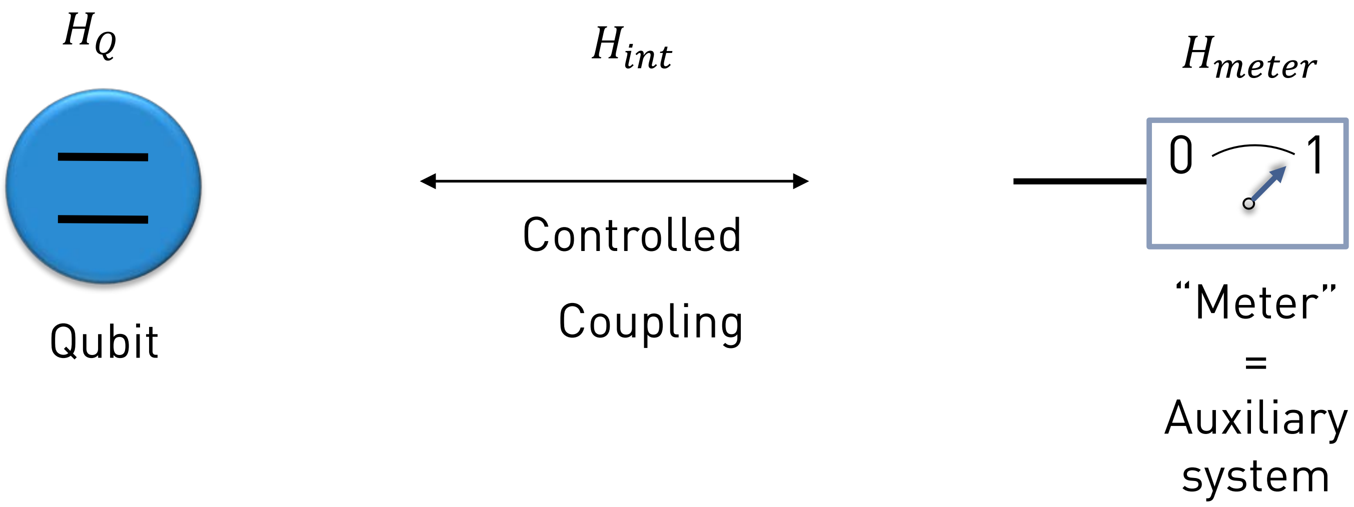

Desirable properties:

- Projective and Quantum non-demolition (QND)
  - Coupling to the meter does not change the state of the qubit $[H_Q, H_{int}] = 0.$
  - Repeated measurement yields the same outcome.
- Good ON/OFF ratio
  - $[H_{int}, H_{meter}] = 0$ during "OFF"
  - $[H_{int}, H_{meter}] \neq 0$ during "ON"
- No spontaneous decay/excitation due to measurement apparatus
- Fast and high fidelity

1. Circuit QED

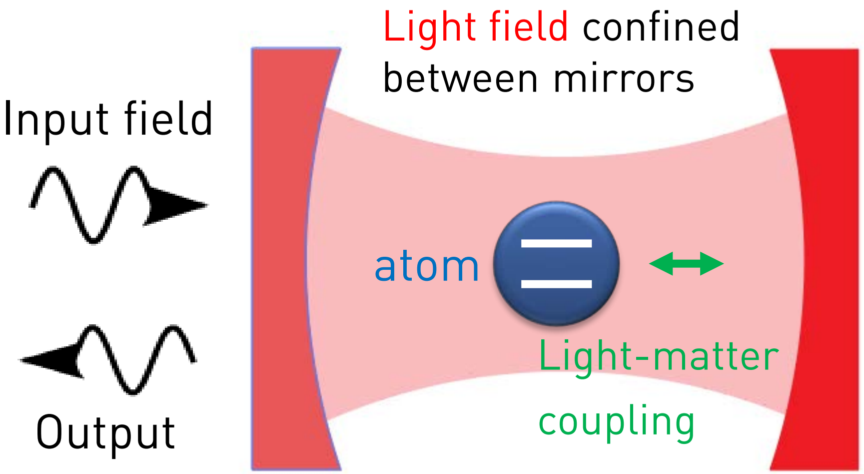

Circuit equivalent

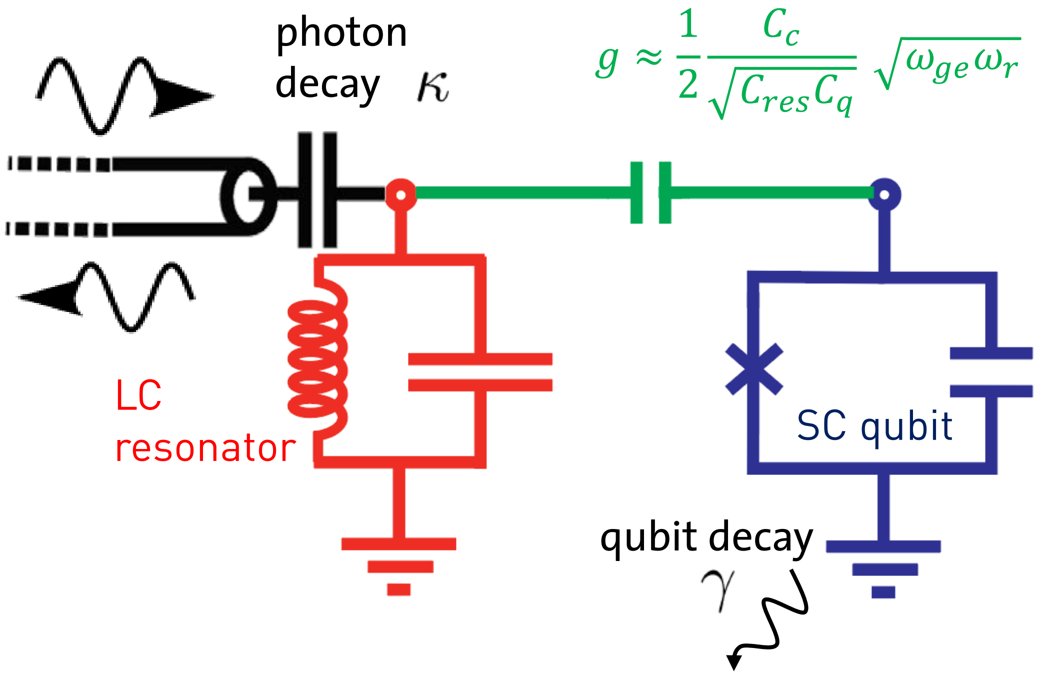

System Hamiltonian (compare chapter 2):

$$H_{\rm sys}/\hbar = \omega_r a^\dagger a \quad + \quad \omega_{ge} b^\dagger b - \frac{\alpha}{2}(b^\dagger)^2 b^2 \quad - \quad g(a - a^\dagger)(b - b^\dagger)$$

$$= \underbrace{\boxed{\omega_r a^\dagger a}}_{\text{Resonator field}} + \underbrace{\boxed{\frac{\omega_{ge}}{2}\sigma^z}}_{\text{qubit}} \underbrace{\boxed{+ g(a^\dagger \sigma^- + a\sigma^+)}}_{\text{coupling}}$$

Jaynes-Cummings Hamiltonian

- Rotating wave approximation (RWA)
- Two-level approximation

S. Haroche & J. Raimond, Exploring the Quantum, OUP Oxford (2006)

1. Circuit QED: Resonant case and dispersive limit

Jaynes-Cummings Hamiltonian:

$$H/\hbar = \boxed{\omega_r a^\dagger a} + \boxed{\frac{\omega_{ge}}{2}\sigma^z} + \boxed{g(a^\dagger \sigma^- + a\sigma^+)}$$

quantized field

qubit

coupling

Strong coupling regime: $g > \gamma,\ \kappa$

Energy level diagram for resonant case $\omega_r = \omega_{ge}$:

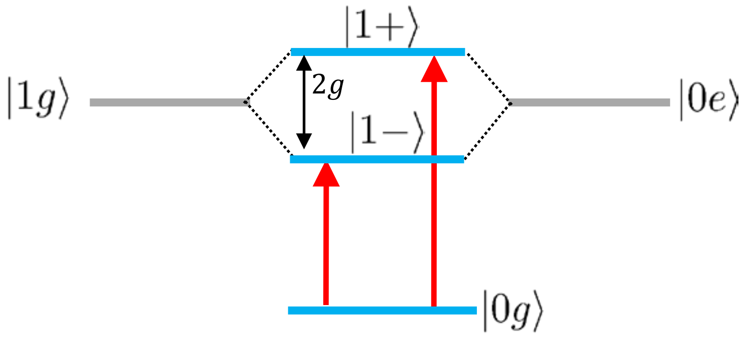

What happens in the limit of large detuning?

$$|\Delta| = |\omega_{ge} - \omega_r| \gg g$$

$$\boxed{\chi \sigma_z a^\dagger a}$$

Dispersive coupling

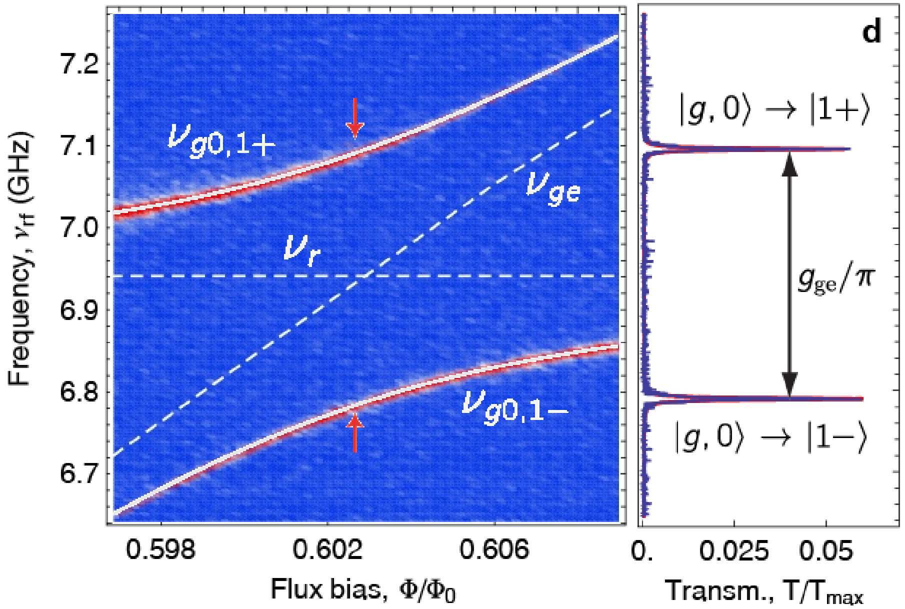

- Limit of large detuning is referred to as the dispersive limit. No resonant exchange of excitations.
- In the dispersive regime coupling Hamiltonian commutes with qubit Hamiltonian.

A. Wallraff *et al.*, *Nature* 431, 162 (2004), J. Fink et al., Nature (London) 454, 315 (2008)

1.4 Principle of Dispersive Qubit Measurement

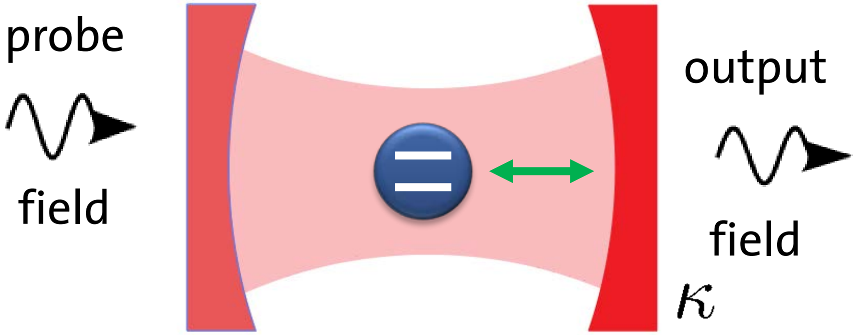

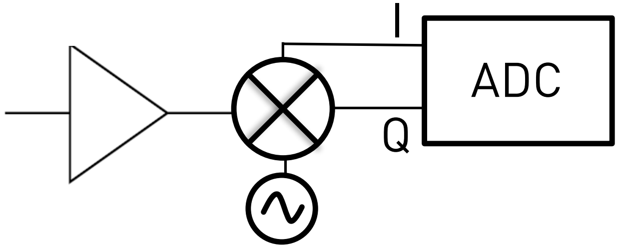

$A\, e^{i\phi} = I + i\, Q$

signal amplitude

Phase

In-phase and quadrature components

In the limit of large detuning $\omega_{\mathrm{r}} - \omega_{ge} \gg g$:

$$H/\hbar \approx (\omega_{\mathrm{r}} + \chi\sigma_z)a^\dagger a$$,with $\chi \approx -\alpha \frac{g^2}{\Delta(\Delta-\alpha)}$

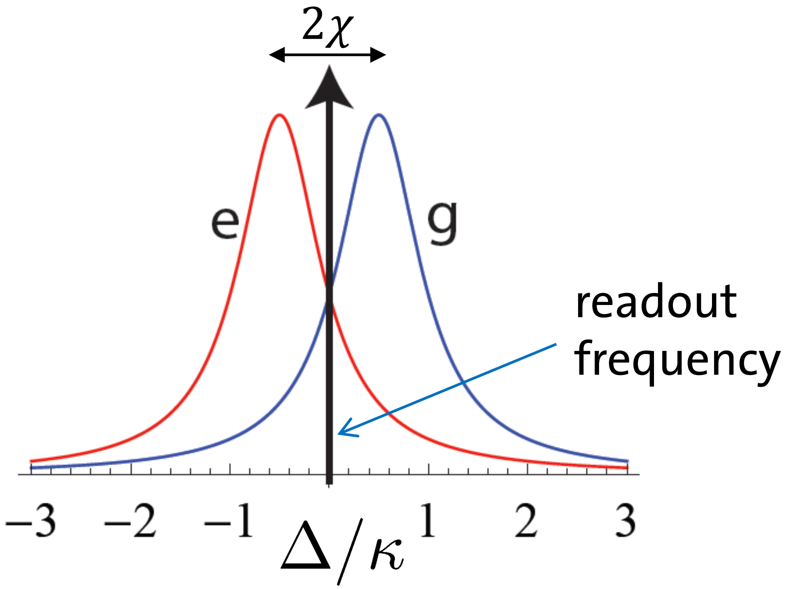

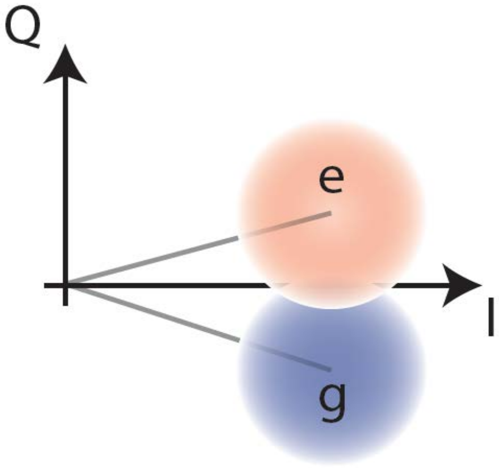

A. Wallraff *et al., Phys. Rev. Lett.* 95, 060501 (2005).
R. Vijay *et al., Phys. Rev. Lett.* 106, 110502 (2011).

1.5 Purcell decay and protection

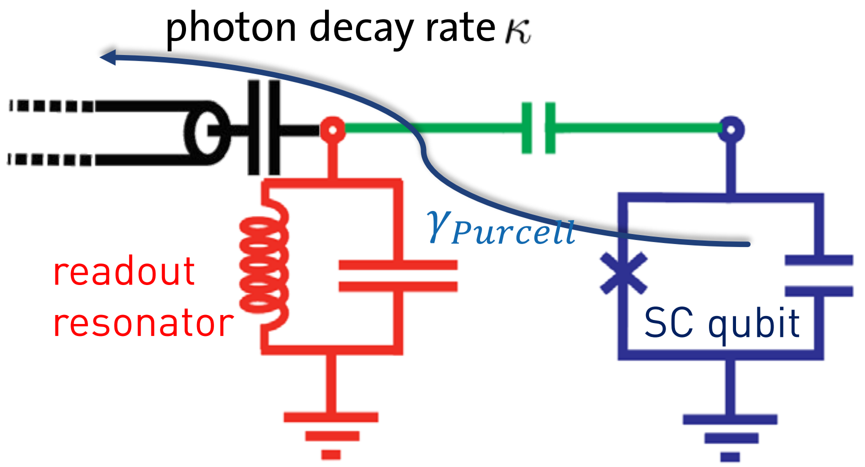

What about decay of the qubit into the measurement line via the resonator?

- In the limit of large detuning we find

$$\gamma_{Purcell} \approx \kappa \frac{g^2}{\Delta^2} \approx \kappa \frac{|\chi|}{\alpha}$$

- Calculate e.g. using the methods discussed in chapter 4.4.
- BUT: Fast readout requires large κ and $|\chi|$.

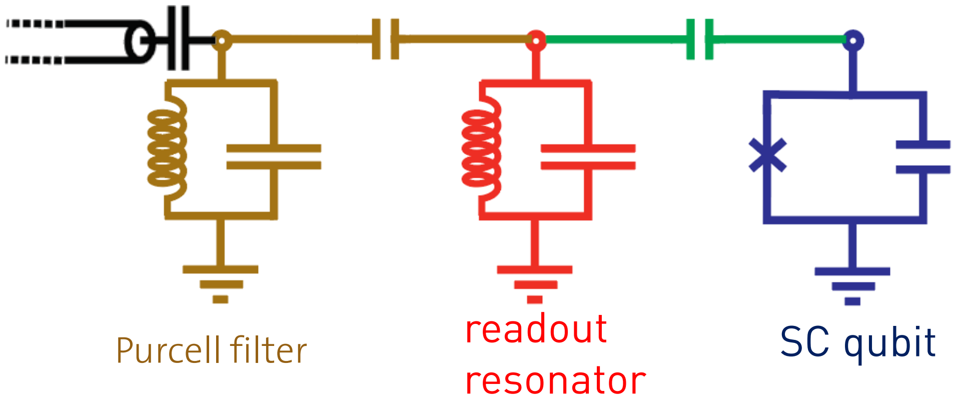

- Solution: Include an additional filter, called "Purcell filter" to suppress qubit decay while allowing for large κ and $|\chi|$.
- Purcell filter can be realized e.g. as an an additional LC- resonator (see schematic).
- In this case

$$\gamma_{Purcell} \propto 1/\Delta^4$$

is strongly suppressed.

Walter et al., *Phys. Rev. Applied* **7**, 054020 (2017)

1.6 Readout Resonator Response

Transmission amplitude or readout resonator extracted through Purcell filter for qubit prepared in ground (g) or excited (e) state :

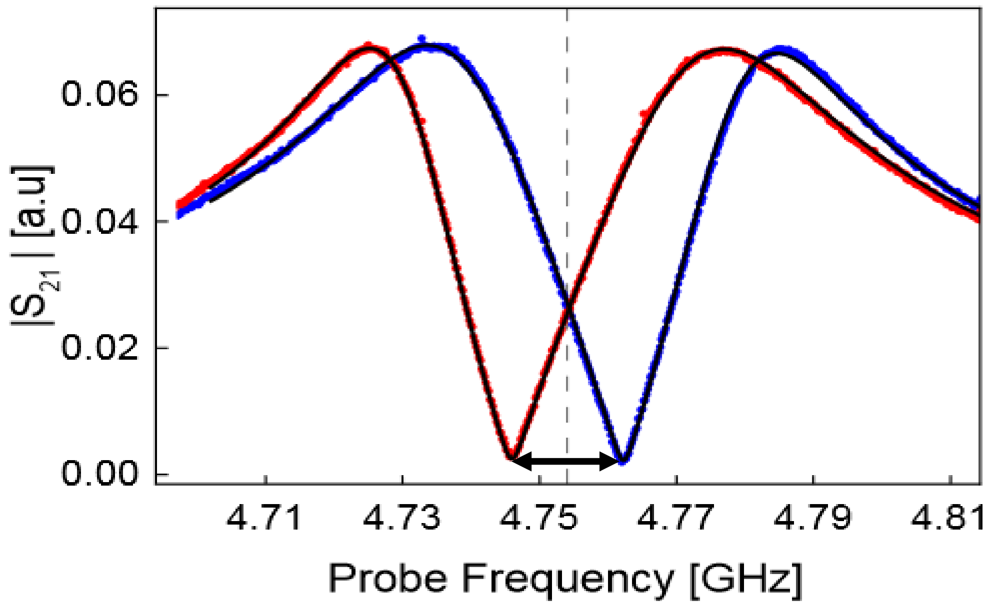

Parameter fit (input-output model):

- Purcell filter $\kappa_p/2\pi$ = 64 MHz
- Readout resonator $\kappa_r/2\pi$ = 37.5 MHz
- State dependent resonator shift $2\chi/2\pi \simeq$ -16 MHz

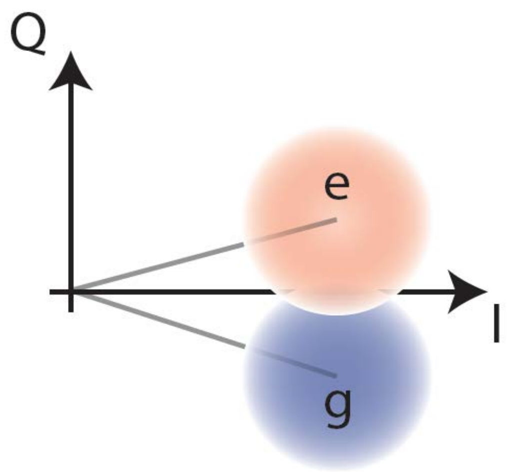

In ground/excited state:

- Data measured after state prep. (*,*)
- Fit to resonator response model (-)

Walter et al., *Phys. Rev. Applied* **7**, 054020 (2017)

Transmon and Readout Circuit optimized for fast Readout

- Transmon qubit
- Qubit drive line
- $\lambda/4$ readout resonator at 4.755 GHz
- $\lambda/4$ Purcell filter at 4.755 GHz
- Measurement input/output line

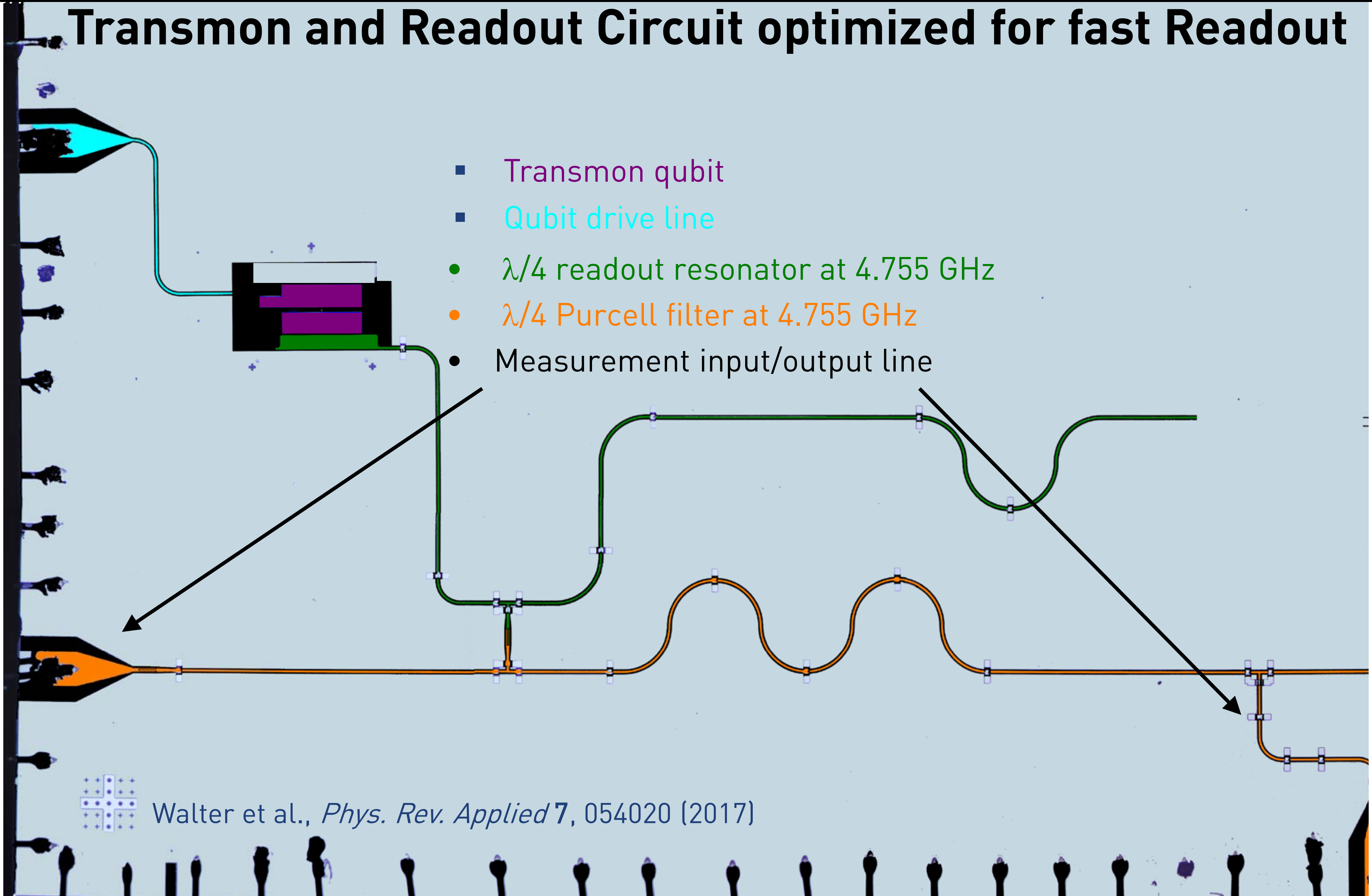

Walter et al., *Phys. Rev. Applied* **7**, 054020 (2017)

1.7 Time Dependence of Measured Quadrature

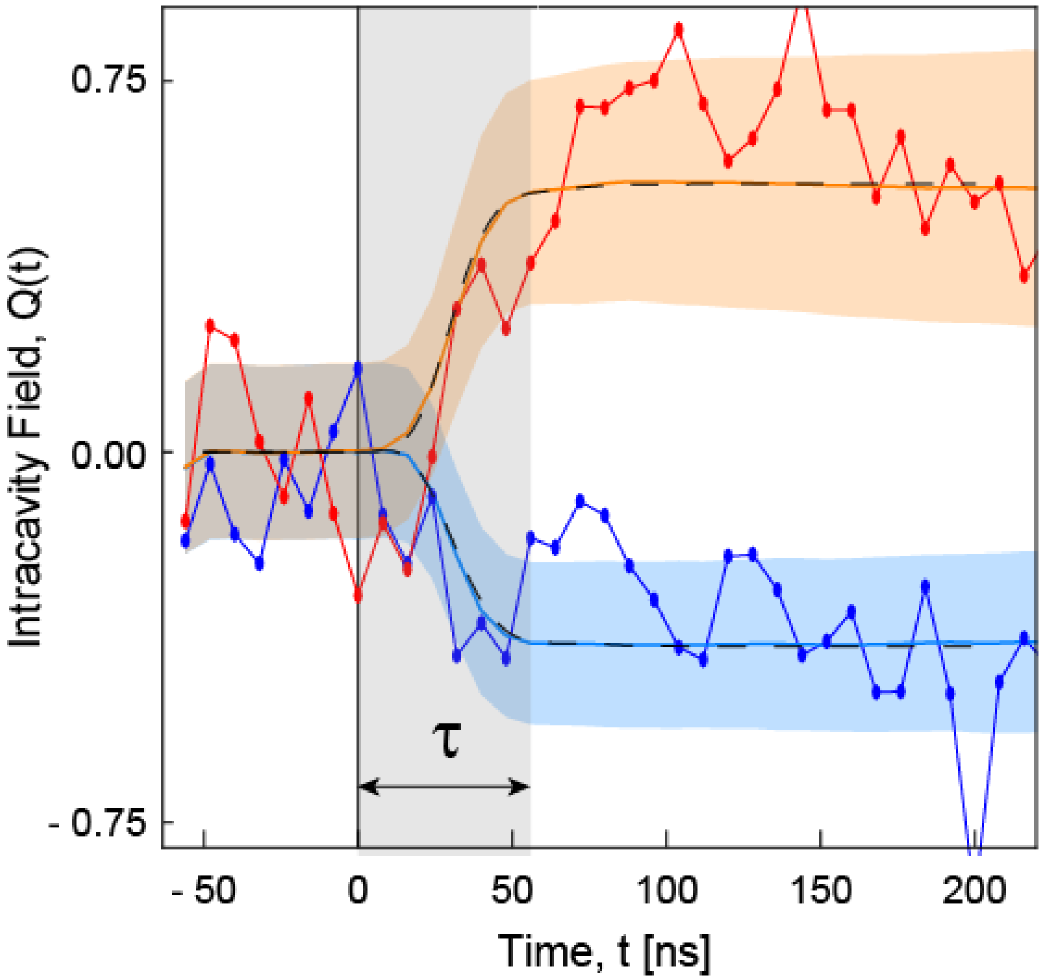

Quantities:

- Single ground state (g) trace
- Average and Stdv of g traces
- Simulated dynamics (-)
- Single excited state (e) trace
- Average and Stdv of e traces
- Simulated dynamics (-)
- Integration time τ

Observations:

- Fast rise of measurement signal (< 50 ns) due large χ (and κ)
- Small decay of average excited state trace due to Purcell protected T_1
- Little increase of average ground state trace due to measurement induced mixing

Walter et al., *Phys. Rev. Applied* **7**, 054020 (2017)

1.8 Histograms of Integrated Quadrature Signals

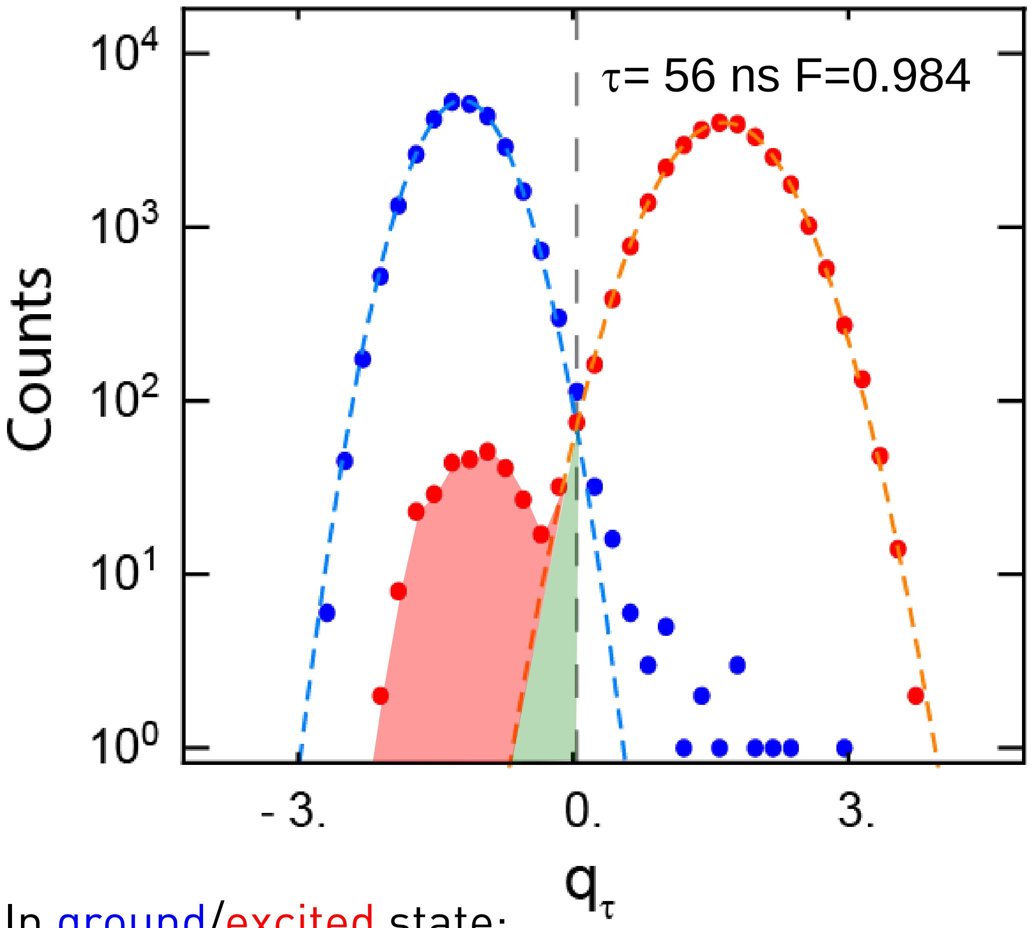

In ground/excited state:

- Data of 30k preparations each (*,*)
- Fitted Gaussian distribution (-,-)
- Constant threshold (---)

Walter et al., *Phys. Rev. Applied* **7**, 054020 (2017)

- Transmission quadrature integrated with opt. filter.
- Definition of errors and fidelities in ground/excited state:
  - Overlap error: $\varepsilon_{o,g/e}$
  - Transition, preparation (and other) errors: $\tilde{\varepsilon}_{g/e}$
  - Total error $\varepsilon_{g/e} = \varepsilon_{o,g/e} + \tilde{\varepsilon}_{g/e}$
- For measurement of unknown state:
  - Total error $\varepsilon = \varepsilon_g + \varepsilon_e$
  - Total fidelity $F = 1 - \varepsilon$

Note:

- Alternative fidelity metric calculates the *average probability of correct assignment*. For a single qubit this probability is $1 - \varepsilon/2$.

.1 Control and Characterization of superconducting qubits

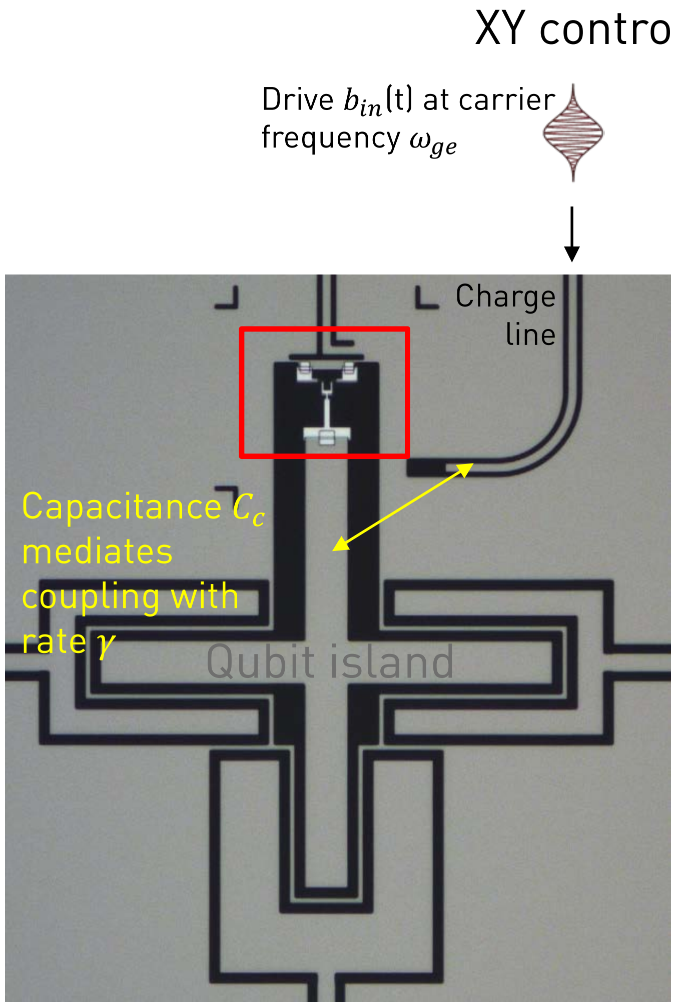

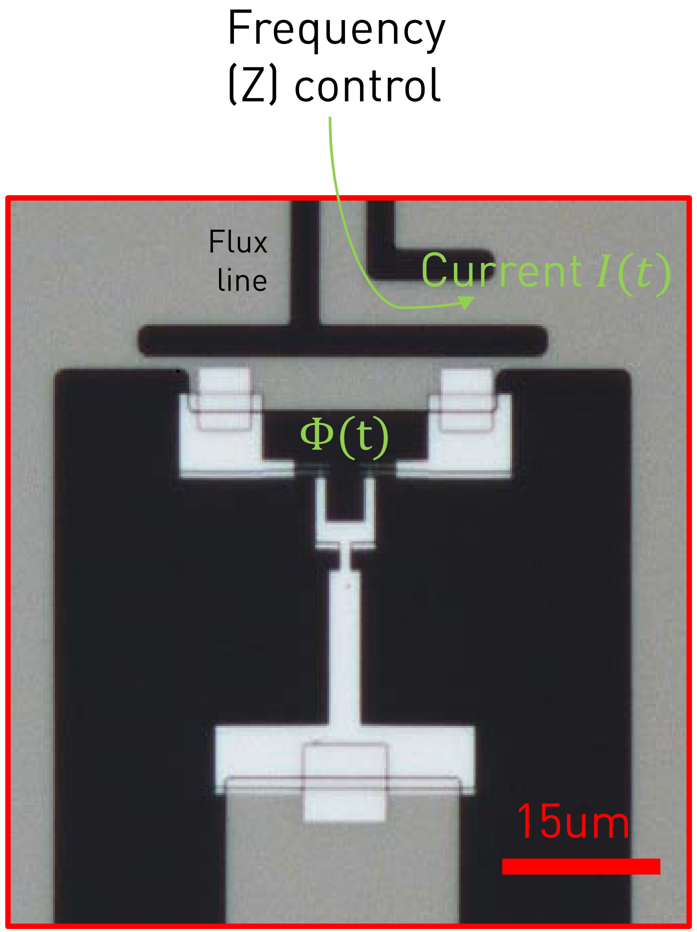

On-chip control

- Microwave drive b_{in}(t) resonant with qubit frequency rotates Bloch vector about X and Y axis. Drive power $P_{in} = \hbar\omega b_{in}^{+} b_{in}$.
- Arbitrary waveform generators (AWG) used to generate pulses, up-converted to the MW frequency band by mixing with a local oscillator field.
- Coupling rate to charge line $\gamma = \frac{C_c^2 Z_0 \omega^2}{C_\Sigma}$ imposes decay and therefore needs to be $\gamma \ll 1/T_1$.
- Tunability of the qubit achieved by sending a current $I(t)$ to a separate control line generating a magnetic flux $\Phi(t)$in the SQUID loop.
- Used for both static (DC) control of the qubit frequency and for applying pulses on nanosecond timescales.

.1 Control and Characterization of superconducting qubits

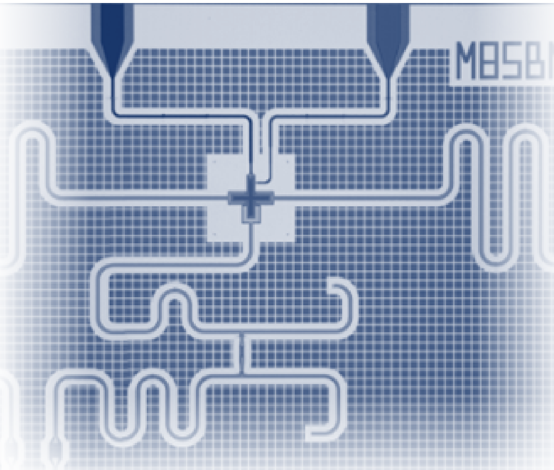

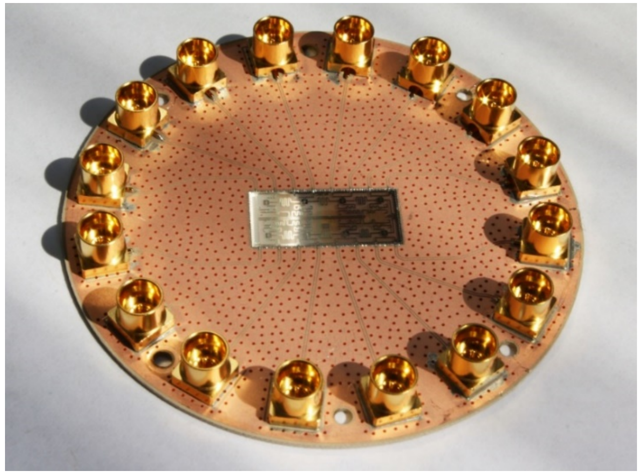

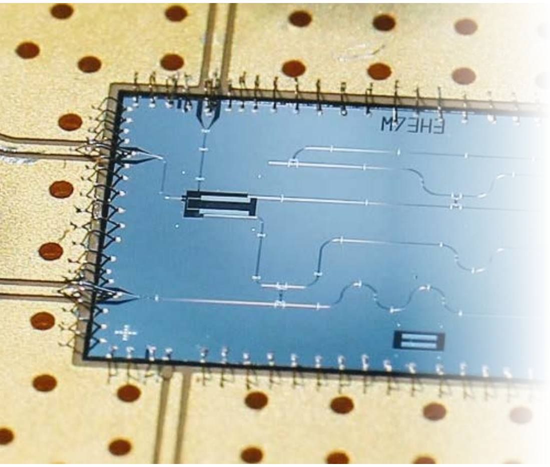

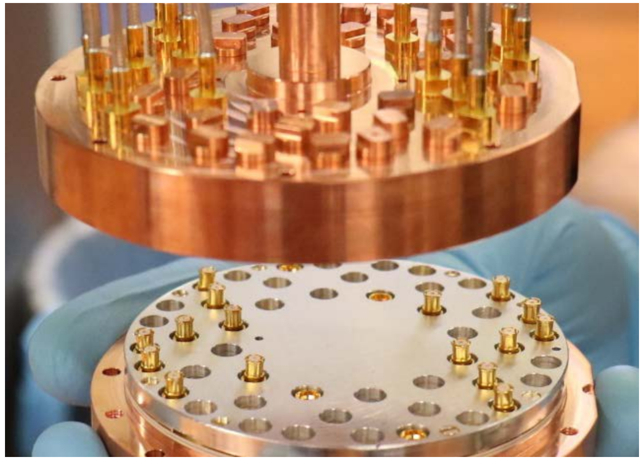

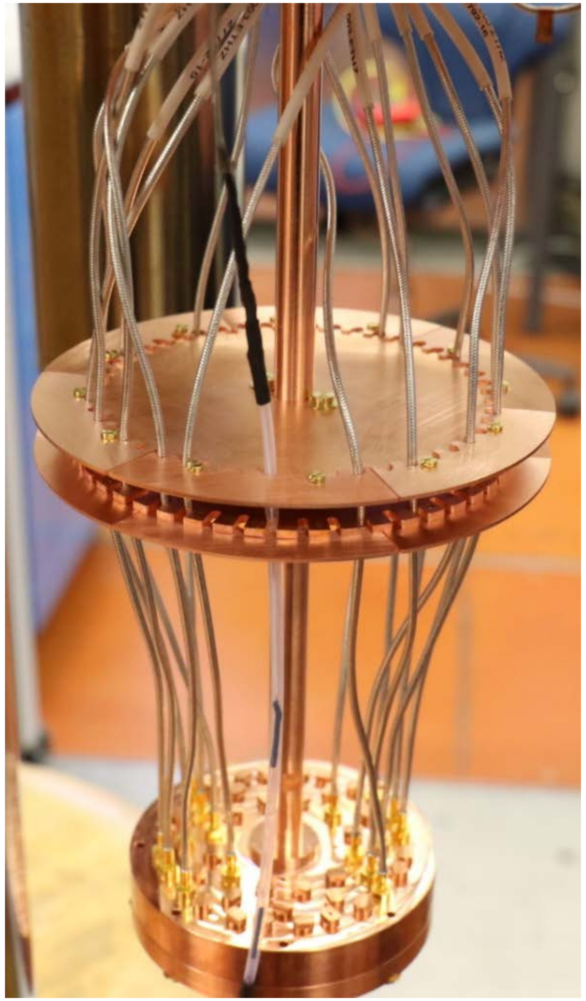

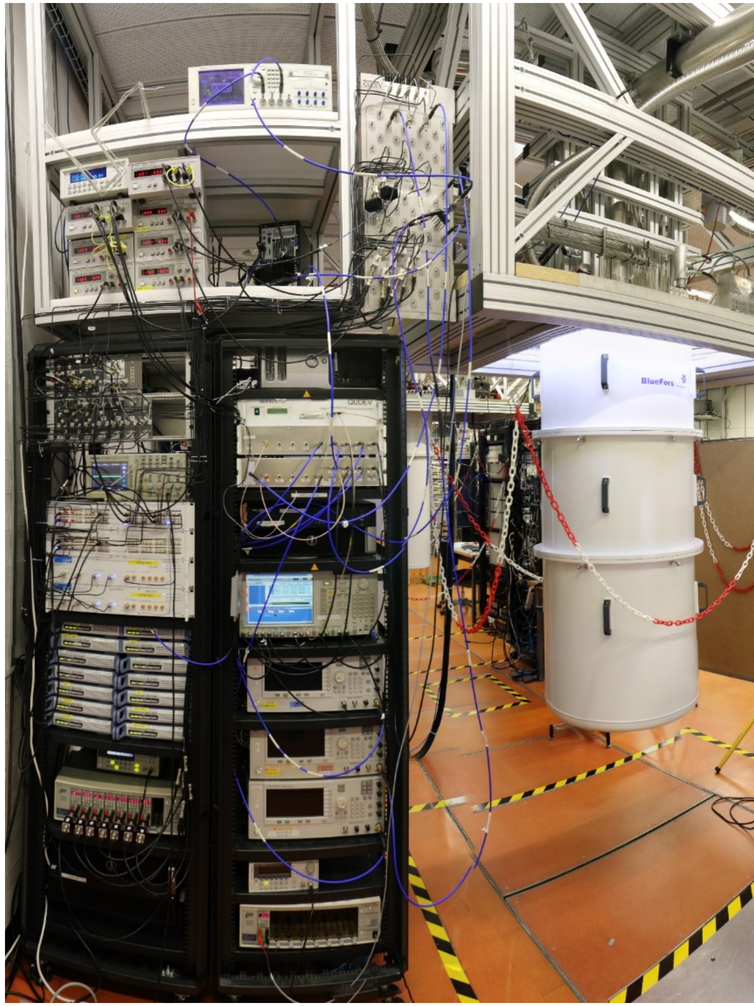

. Measurement of Rabi oscillations

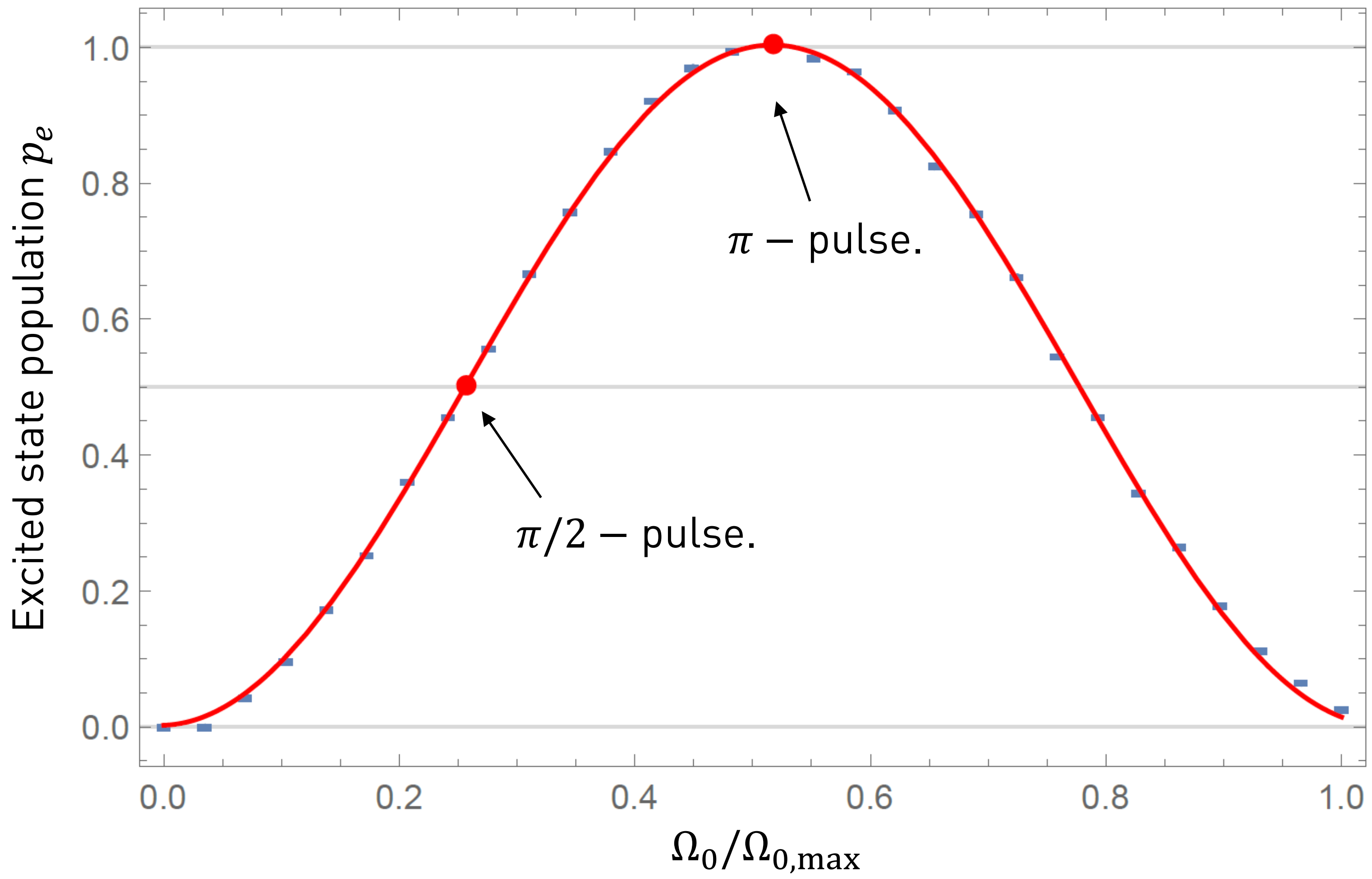

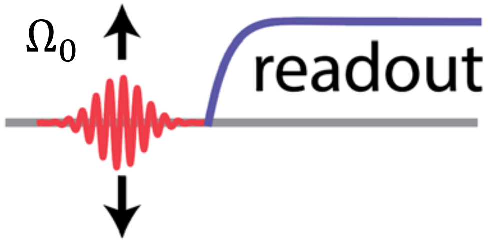

- Qubit frequency $\omega_{ge}/2\pi = 5.758$ GHz determined spectroscopically.
- Initialize qubit in ground state.
- Apply pulse at ω_{ge} with variable amplitude Ω_0.
- Gaussian pulse envelop with characteristic $\sigma \sim 5 - 10ns$.
- Readout qubit state and average over ~10^3 repetitions.
- Sinusoidal fit to extract π- and $\pi/2$-pulse amplitude.

Rabi oscillations

How does this look like?

$$P_{g\to e}(t) = \left(\frac{\Omega_1}{\Omega}\right)^2 \sin^2\left(\frac{\Omega}{2}t\right)$$ with the generalized Rabi frequency $$\Omega = \sqrt{\Delta^2 + \Omega_1^2}$$

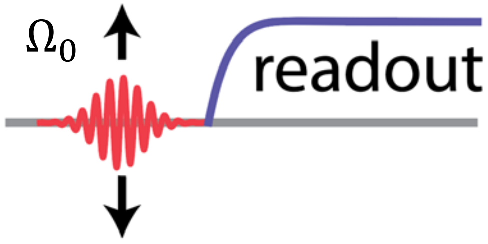

(i) Probability vs. time:

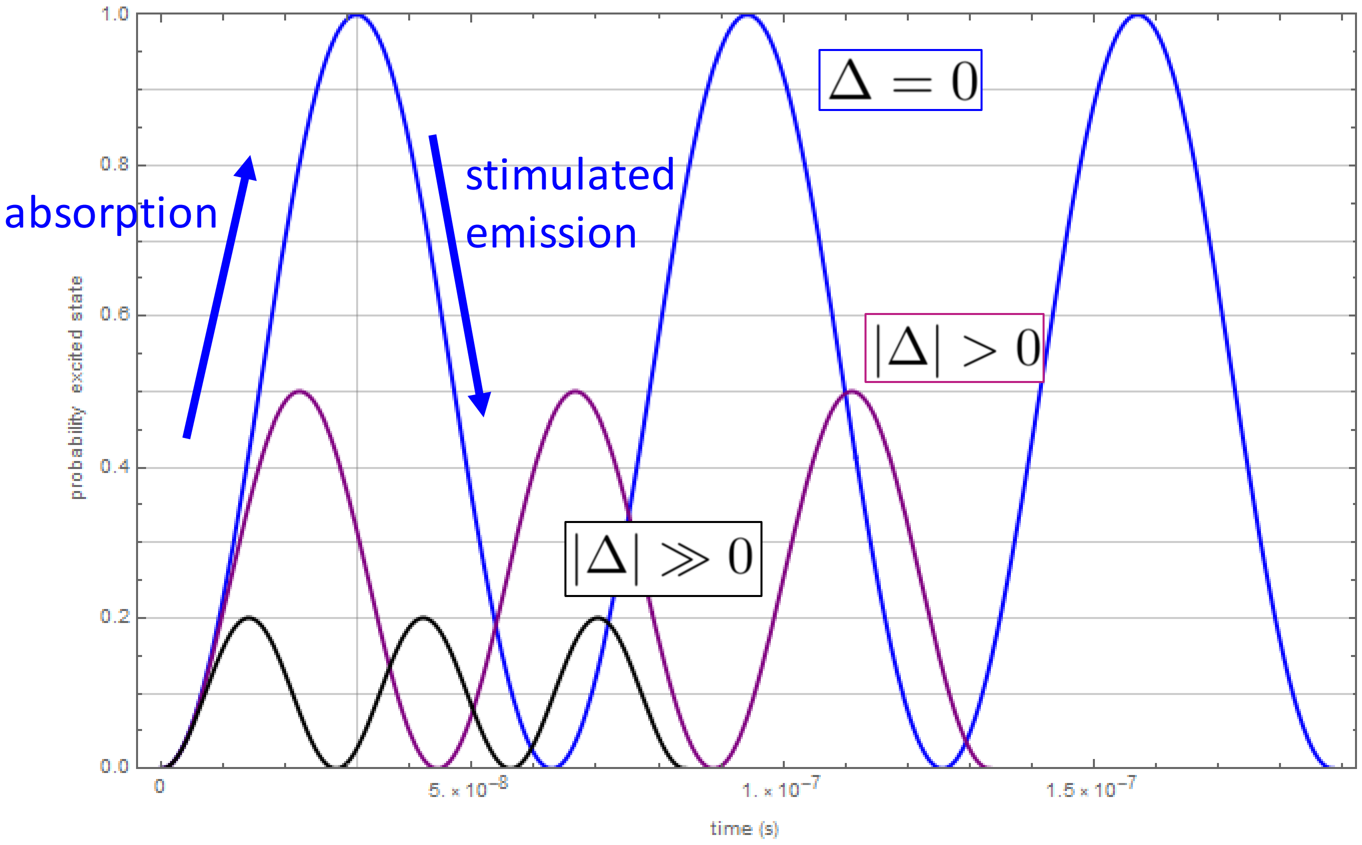

- Qubit frequency $\omega_{ge}/2\pi = 5.758$ GHz determined spectroscopically.
- Initialize qubit in ground state.
- Apply pulse at ω_{ge} with variable amplitude Ω_0.
- Gaussian pulse envelop with characteristic $\sigma \sim 5 - 10ns$.
- Readout qubit state and average over ~10^3 repetitions.
- Sinusoidal fit to extract π- and $\pi/2$-pulse amplitude.

. Measurement of relaxation time

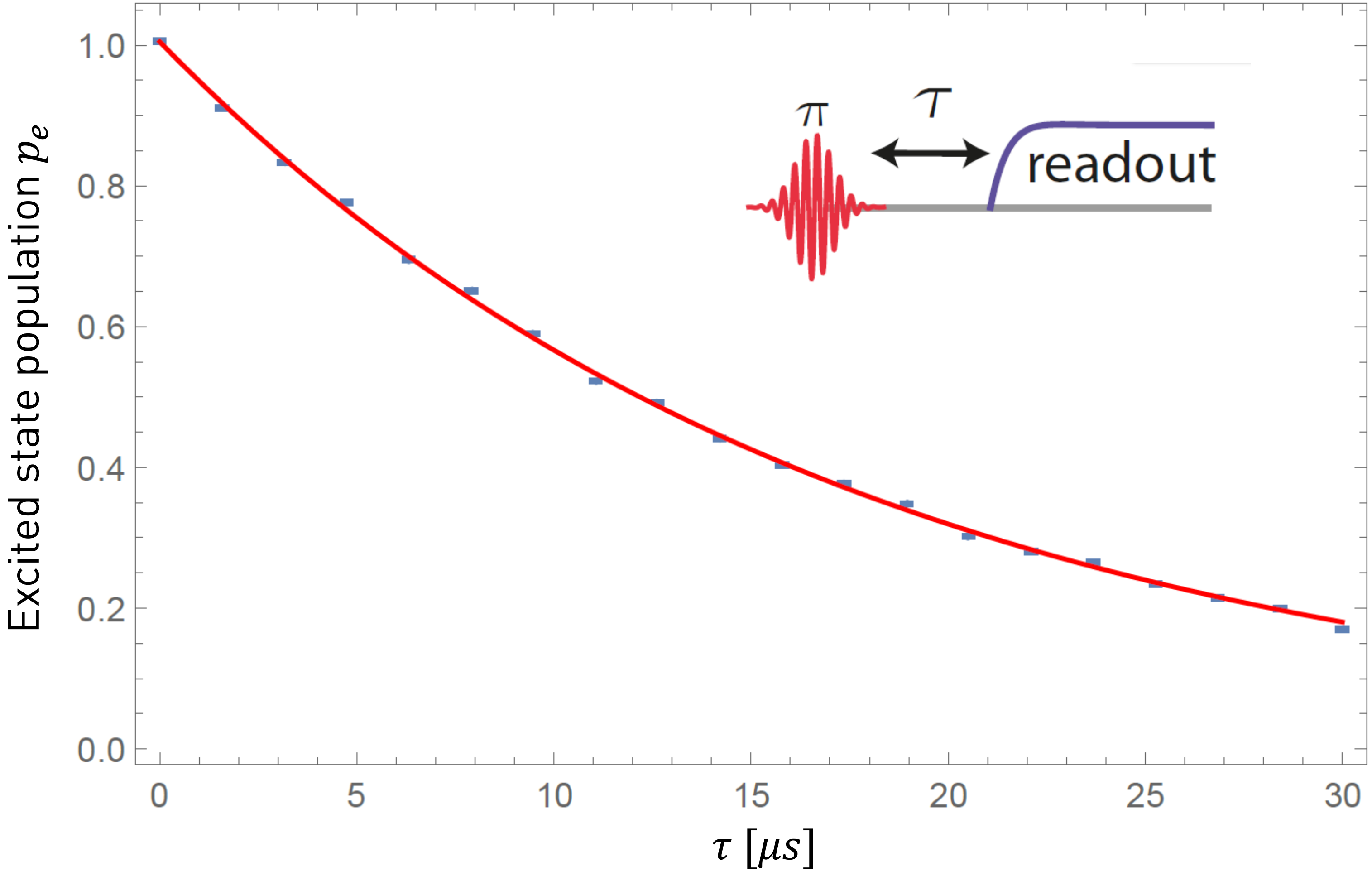

- Excite qubit with an initial $\pi -$ pulse.
- Wait variable time τ before measuring the qubit population.
- Fit exponentially decaying function to extract relaxation time $T_1 \approx 18\ \mu s$.

.4 Measurement of dephasing time

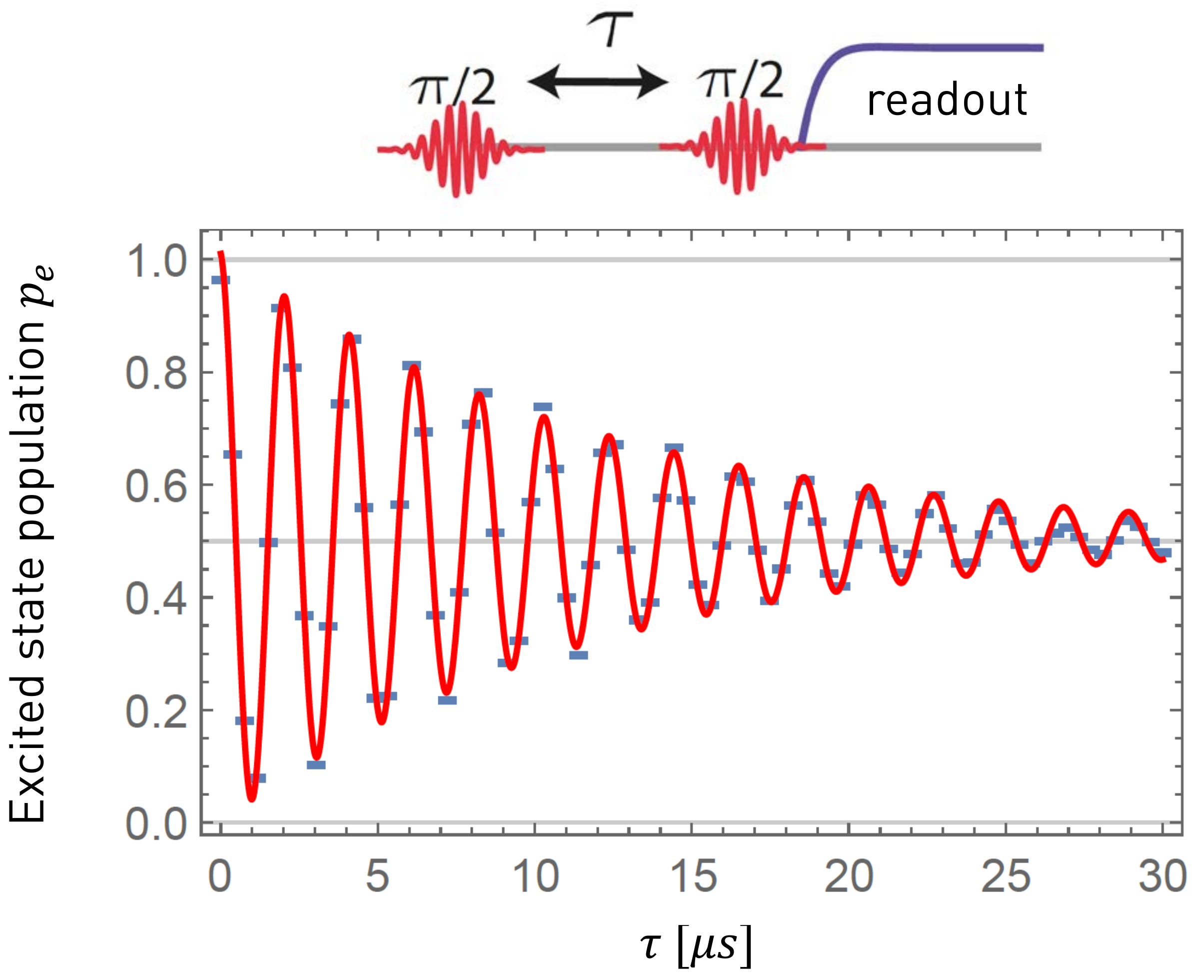

- Initial $\frac{\pi}{2}$-pulse prepares $|g\rangle + |e\rangle$.
- Map remaining coherence after time τ to excited state using a second $\frac{\pi}{2}$- pulse, and measure.
- Detune pulse by $\mathrm{f_{IF}} = 0.5$ MHz from qubit frequency to obtain oscillating pattern. → Higher accuracy in estimating the qubit frequency.
- Fit Characteristic decay time $T_2^* = 13\ \mu s$
- In this case, decay reasonably well described by exponential function $e^{-\tau/T_2^*}$
- Depending on spectral properties of the dominant noise source, decay better described by different functional form, e.g. Gaussian decay for 1/f – noise.
- If relaxation is only source of decoherence: $T_2 = 2\,T_1$ ("T1 limit of dephasing time").

Ithier, G. et al. PRB 72, 134519 (2005).

.4 Measurement of dephasing time

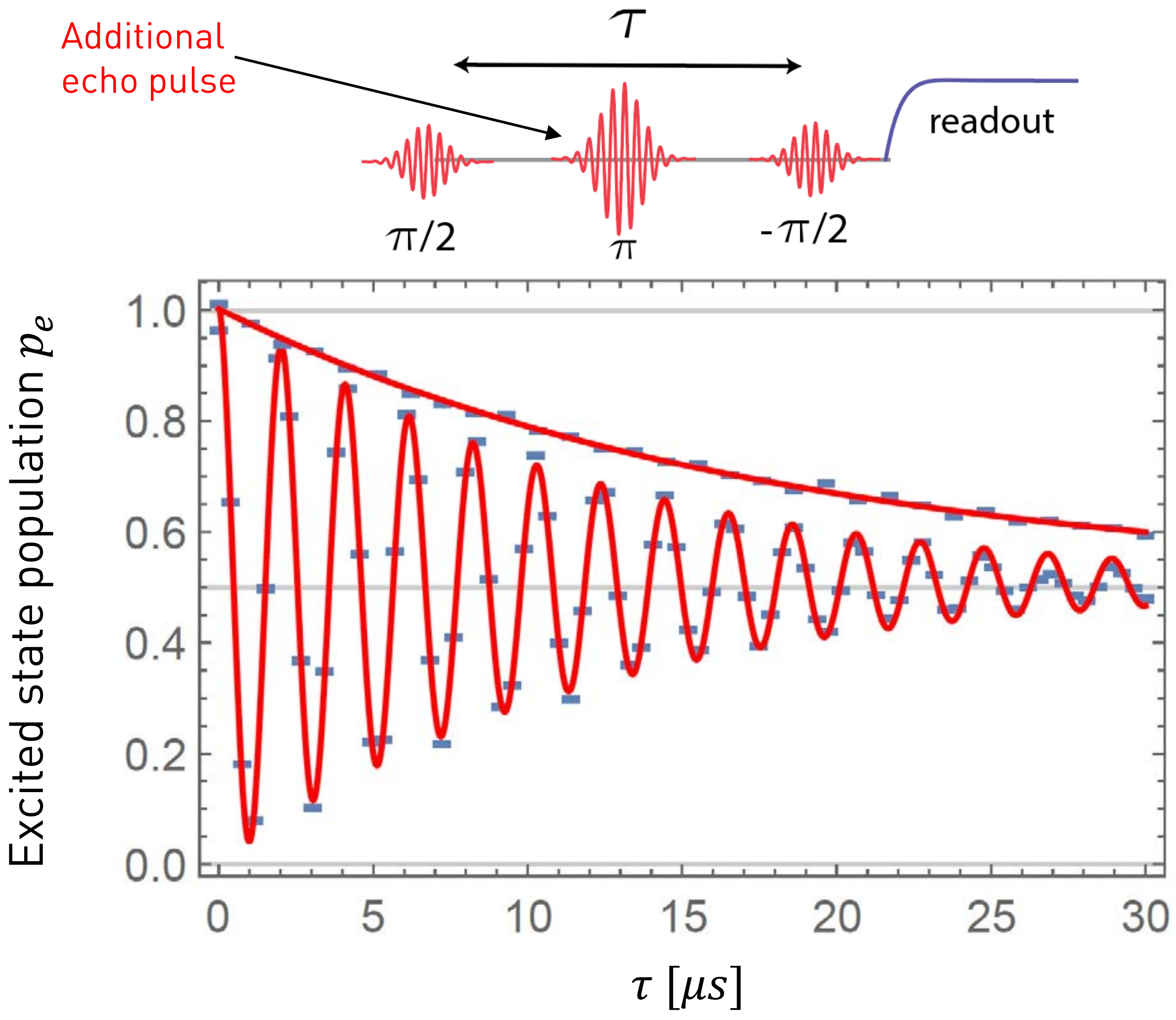

- Low frequency noise can be partly compensated for by applying an echo π-pulse after $\tau/2$ to reverse the direction of the Lamor precision.
- The resulting decay time $T_2^{echo} = 18\ \mu s$ is longer than T_2^*.
- Explanation: Low frequency noise which causes the qubit frequency to change on timescales longer than τ_{max} will cancel out.
- Variants of such dynamical decoupling sequences can be used to do noise spectroscopy → See e.g*. Bylander et al., Nat. Phys. (2011)*

Ithier, G. et al. PRB 72, 134519 (2005).

. Sources and mitigation of noise: A few examples

Relaxation mechanisms (T_1)

1) Radiative decay and ohmic loss due to coupling of the qubit to the electromagnetic environment.

2) Coupling to material defects described by two-level systems (TLS) mostly at the material interfaces

3) Relaxation induced by quasiparticle tunneling

4) Other sources, e.g. vortex dynamics.

Dephasing mechanisms (T_2)

1) Photon shot noise through dispersively coupled elements, e.g. residual photons in the readout circuit.

2) Magnetic flux noise in flux-tunable qubits.

3) Charge noise in combination with charge dispersion of transmon energy levels.

.1 Characterization & Benchmarking of Quantum Processes

Ideally

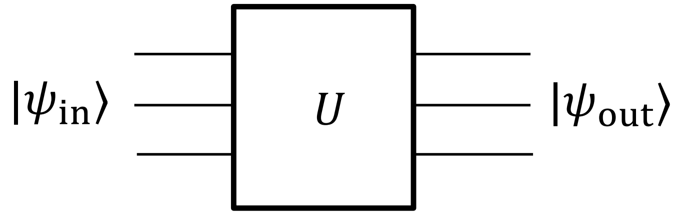

Realistically

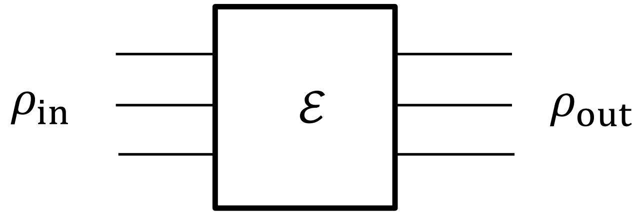

Questions:

- General properties of the map $\mathcal{E}$?
- How to measure the map $\mathcal{E}$?
  - State and process tomography
- Measure of distance between quantum states and processes: Fidelity
- How to benchmark quantum gates with fidelities close to one?
  - Randomized Benchmarking

State tomography: Example Bell state

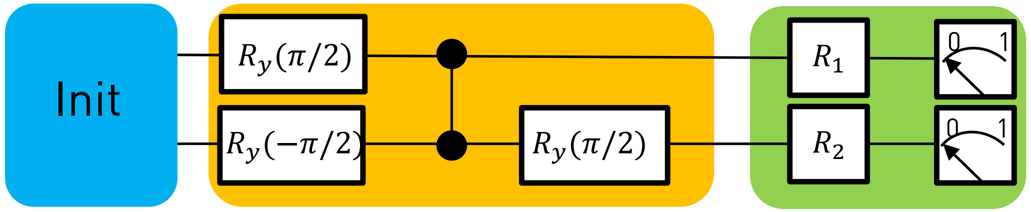

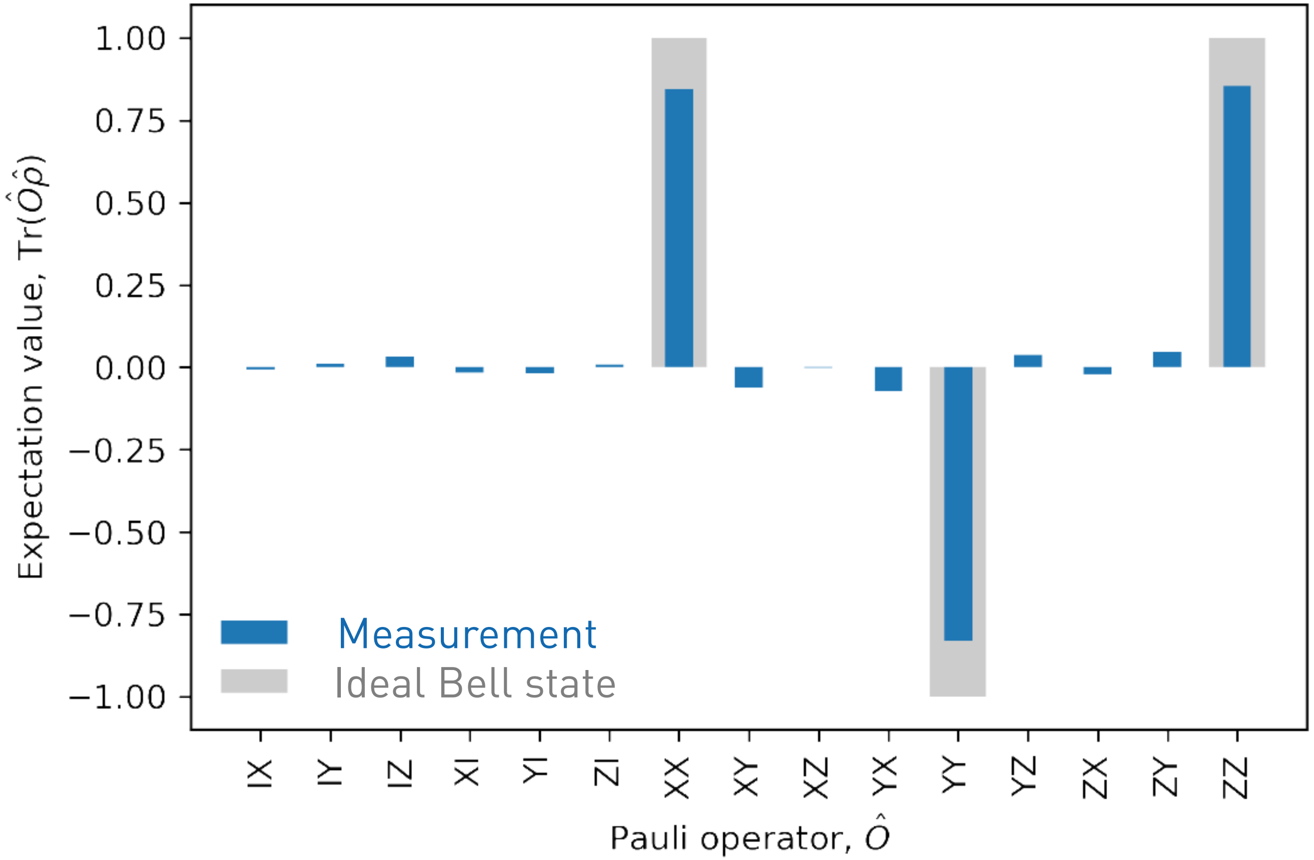

- Initialize qubits in ground state
- Prepare Bell state
- Apply basis rotation pulses R_i to to effectively measure along x, y, z axes.
- Observations
  - Single-qubit expectations vanish. Characteristic feature of entangled Bell state.
  - Measured XX, YY, ZZ correlations exhibit reduced contrast compared to ideal state.
  - Deviations from ideal state due to (i) finite state preparation error and (ii) finite measurement fidelity.

How to account for finite readout efficiency?

. State tomography: Finite readout fidelity

Readout assignment probability matrix M

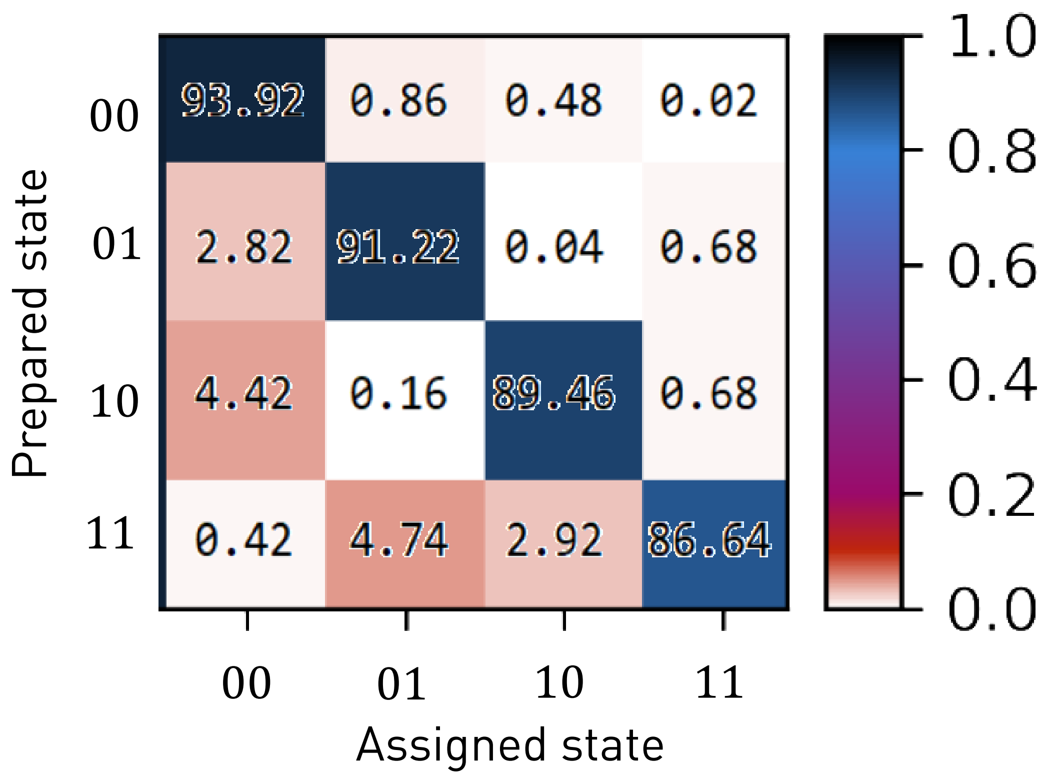

- Possible measurement outcomes $i \in \{00,01,10,11\}$.
- Assume an unknown state with measured probabilities p_i to obtain one of the four possible outcomes.
- Use assignment probability matrix M to estimate

$$\tilde{p}_i = \sum_j M_{ij}^{-1} p_j$$

Probabilities compensating for finite readout fidelity.

Multiplication with inverse assignment probability matrix

Measured probability to be in state i.

- Comments:
  - Relies on the assumption that ideal reference states can be prepared.
  - In general, need MLE to ensure positivity of $\tilde{p}$.

.4 State tomography: Mostly likely density matrix

Pauli set after compensating for readout infidelity.

- Expectation values based on $\widetilde{p_i}$ display larger contrast.
- All expectation values are close to target, indicating small errors in the Bell state preparation.

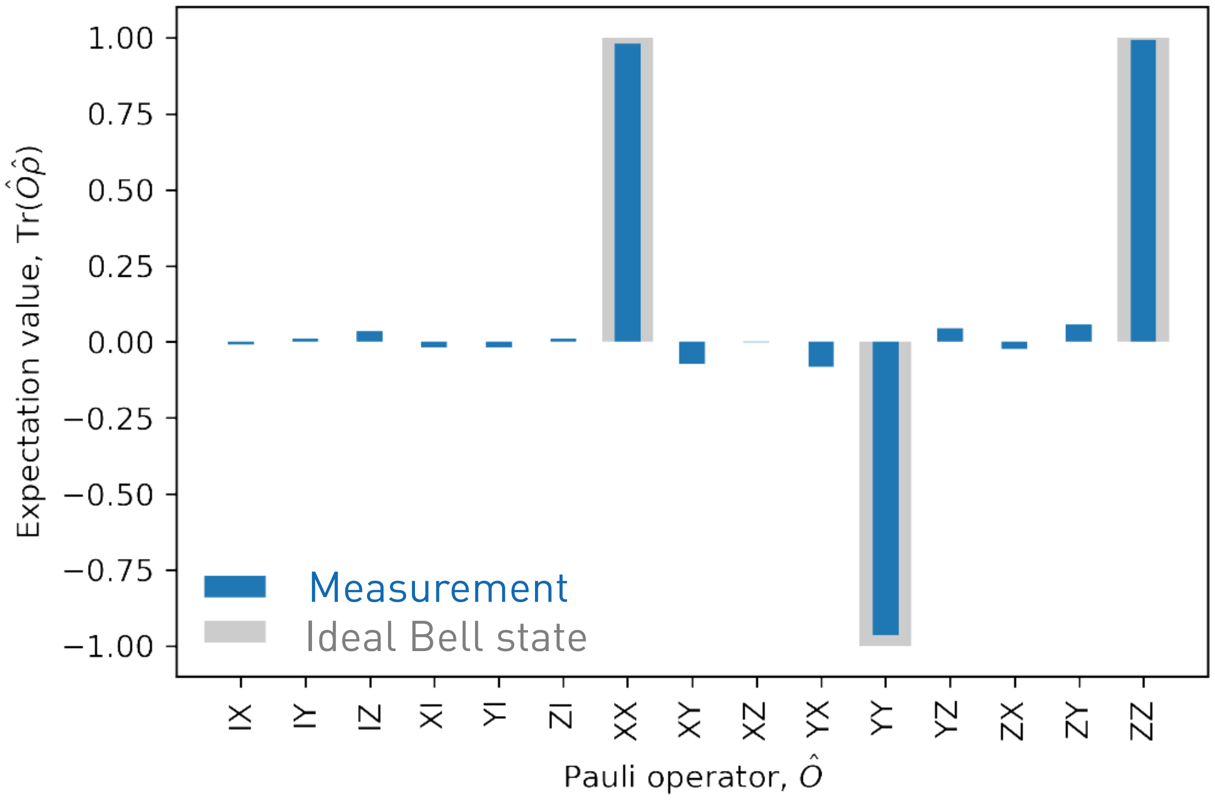

Density matrix reconstruction

- Minimize negative Log-likelihood function, subject to the constraint that ρ has positive eigenvalues.
- Fidelity $F = \sqrt{\langle\psi|\rho|\psi\rangle} = 0.98$

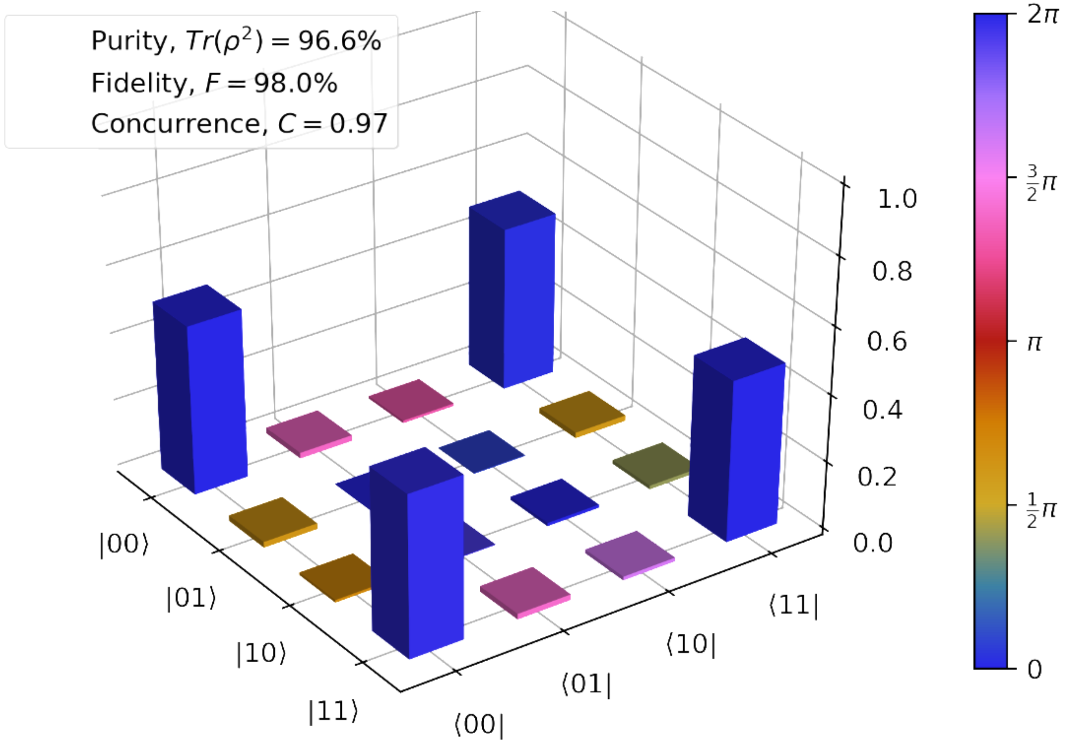

. Process tomography

One possible representation of a quantum process: Pauli transfer matrix $\mathcal{R}$.

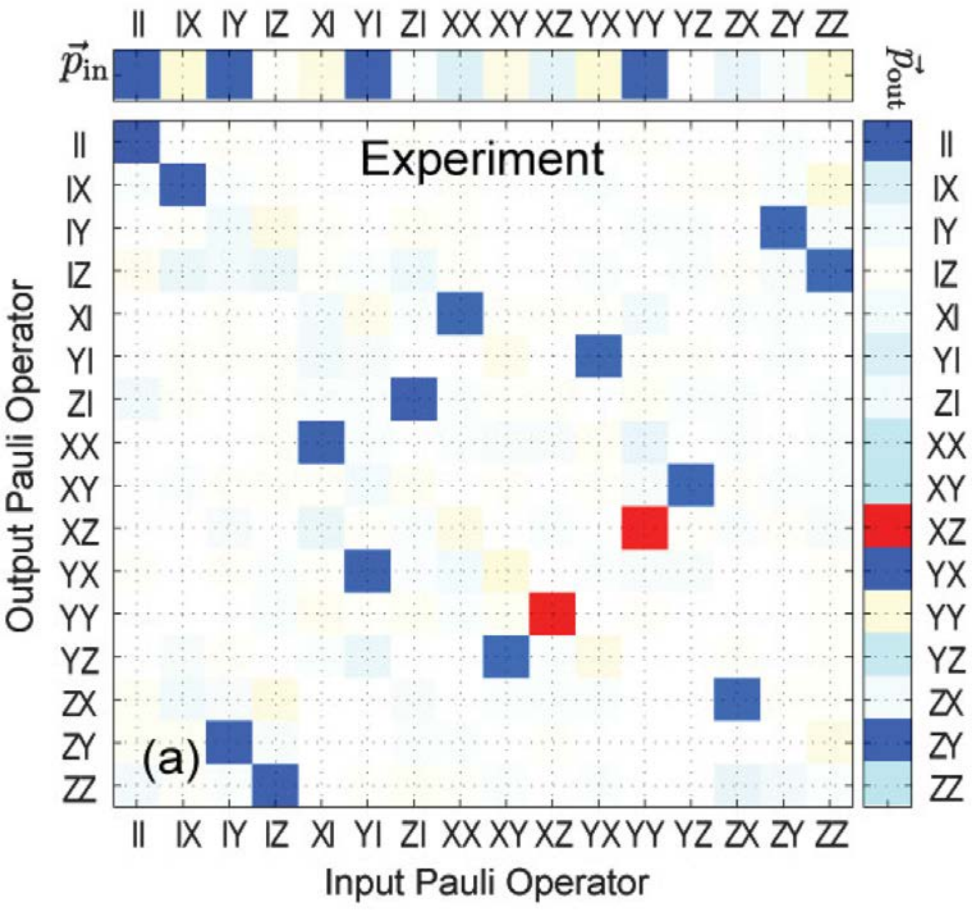

Figure from Chow et al., 109, 060501 PRL (2012)

- Concept of Bloch vector $\vec{r}$ can be generalized to multi-qubit states.
- Elements of $\vec{r}$ are given by muti-qubit Pauli expectation values $\langle\sigma_{i_1}\sigma_{i_2} \dots\rangle$ with $\sigma_i \in \{I, X, Y, Z\}$, which fully characterize a quantum state.
- Pauli transfer matrix specifies quantum process by relating arbitrary input Bloch vector to the corresponding output Bloch vector according to
$$\vec{r}_{out} = \mathcal{R}\,\vec{r}_{in}$$
- Example shows most likely R measured in an experiment for a CNOT gate.
- Process fidelity, computed as $F = \frac{\mathrm{Tr}[\mathcal{R}_{ideal}^T\mathcal{R}]/d+1}{d+1}$,corresponds to average fidelity of output state.

State and process tomography: Discussion

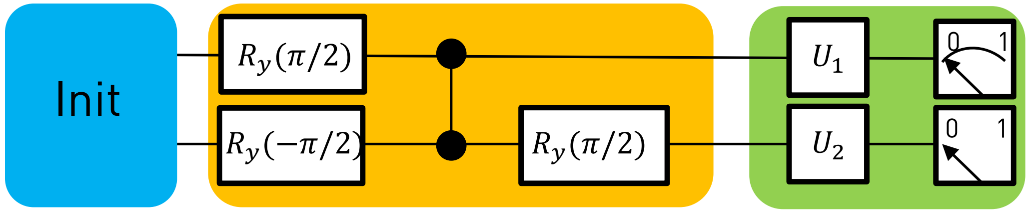

- Result of a tomographic measurement is sensitive to "state-preparation and measurement" (SPAM) errors.
- For processes, e.g. gates, which are very close to target, it can be challenging to distinguish errors in the process from SPAM errors.
- How to quantify the (small) errors in a process/gate in the presence of finite initialization and readout fidelity?
- Strategy: Amplify errors by applying sequences of multiple gates before measurement.
  - Additional advantage: Tests how repeatable operations are.
- → Widely used approach: Randomized benchmarking.

. Randomized benchmarking

- For simplicity, consider single-qubit case.
- Apply sequence of n gate operations U_i before measuring.

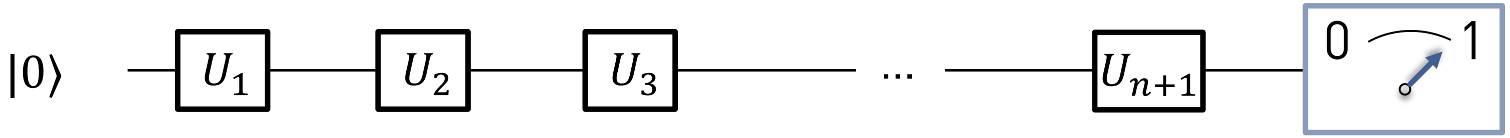

- Gates U_i are chosen randomly from the Clifford group, mapping an element of the Pauli group to an element of the Pauli group. For a single qubit there are 24 Clifford gates.
- Last gate U_{n+1} is chosen such that in the absence of errors state is brought back to initial state, i.e. $U_{n+1} \dots U_2 U_1 = I$.
- Average over m different such sequences.
- Success probability p_0 to recover the initial state decays exponentially with # of gates $p_0 \propto \alpha^n$, with depolarization parameter α.
- The error per gate is given by $\epsilon_{RB} = (1-\alpha)\frac{(d-1)}{d}$ where d is the dimension of Hilbert space (d=2 for a single qubit).

Knill et al., PRA **77**, 012307 2008

Randomized benchmarking: Example single qubit gates

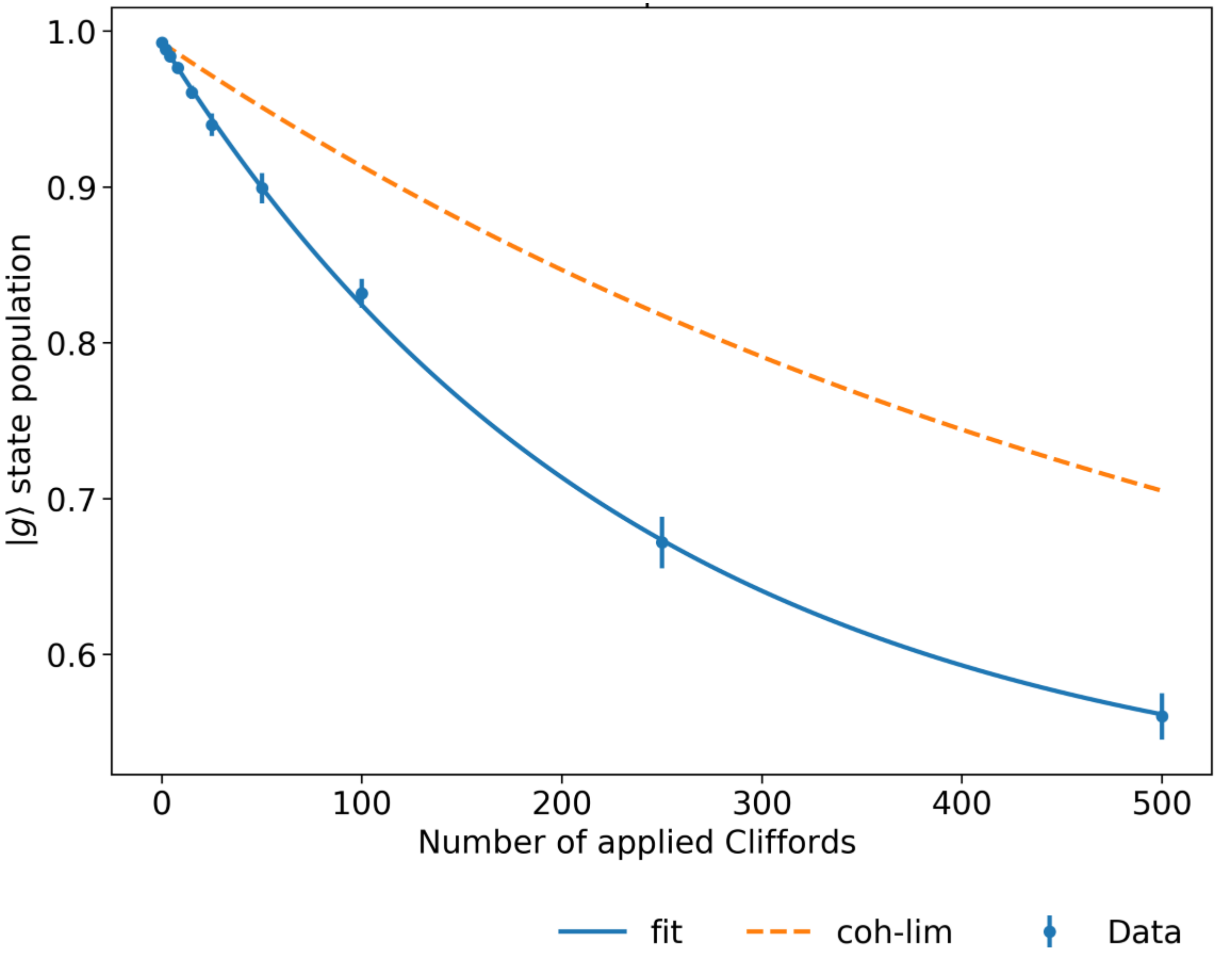

- Pulse duration typically between 15 to 50 ns. Leakage into second excited state avoided by using (DRAG*) pulse parametrization.
- Use Clifford decomposition in terms of X rotations and virtual Z gates (see McKay et al., PRA (2017)).
- Population of ground state decays exponentially.
- Fitted depolarization parameter $\alpha \approx$99.6% and gate error $\epsilon \approx 0.2\%$ in this example.
- Orange dashed line indicates the limit expected when only considering qubit decoherence.
- Deviation from coherence limit hints at finite control errors, e.g. resulting in leakage to the f-level.

*Motzoi et al., PRL 103, 110501 (2009)

. Interleaved Randomized benchmarking (IRB)

Question how to characterize the fidelity of one particular Clifford gate V?

- Compare decay of standard RB sequence …

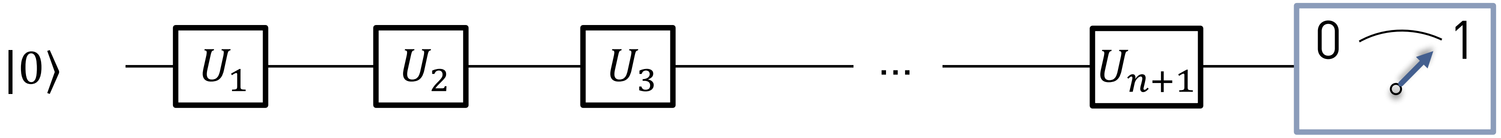

- …with result of a 2nd experiment, in which gate V gets interleaved with random Clifford gates.

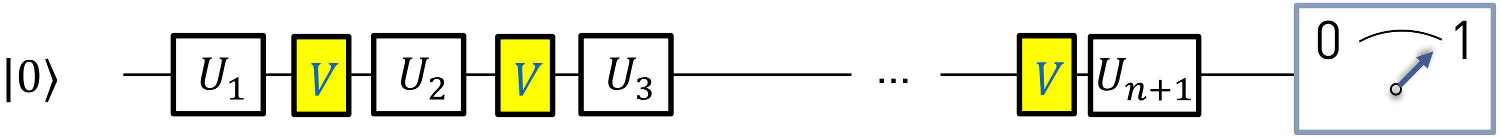

- Difference between the depolarization parameters α_{RB} and α_{IRB} results in an estimate for the error $\epsilon_V = \frac{d}{d+1}(1 - \frac{\alpha_{IRB}}{\alpha_{RB}})$ per gate V.

- Randomized Benchmarking can be generalized to multi-qubit gates.

Magesan et al., PRL 109, 080505 (2012)